On the unoccupied electronic states of vanadium diselenide

1991 J. Phys.: Condens. Matter 3 813

(http://iopscience.iop.org/0953-8984/3/7/006)

J. Phys.: Condens. Matter 3 (1991) 813–825. Printed in the UK

On the unoccupied electronic states of vanadium diselenide

A R Law†§, P T Andrews† and H P Hughes‡

† Department of Physics, University of Liverpool, Oxford Street, PO Box 147, Liverpool L69 3BX, UK

‡ Physics and Chemistry of Solids Group, Cavendish Laboratory, Madingley Road, Cambridge CB3 0HE, UK

Received 20 July 1990, in final form 6 November 1990

Abstract. The unoccupied electronic states of the group Vb transition metal dichalcogenide compound vanadium diselenide have been measured up to about 10 eV above the Fermi level using isochromat momentum-resolved inverse photoemission. Bands along the ΓA direction of the Brillouin zone were probed by recording normal-incidence spectra at photon energies between 17 and 28 eV. Band dispersions in the two principal symmetry planes of the Brillouin zone, ΓALM and ΓAHK, were determined from off-normal-incidence spectra recorded at a photon energy of 20 eV. Strong features resulting from transitions into the unoccupied V 3d-derived bands are seen at about 1 eV and about 3 eV above the Fermi level; the variation of the intensity of these features with the azimuthal angle of electron incidence reflects the three-fold symmetry of the 1T crystal structure adopted by VSe_2. A broad feature centred at about 8 eV, and showing an onset at about 6 eV, is associated with higher-lying s/p bands while a weak peak at about 5 eV, which shows no dispersion along ΓA, is tentatively identified as a surface resonance. The results are compared with published band-structure calculations.

1. Introduction

The quasi-two-dimensional transition metal dichalcogenide compounds (TMDCs), MX_2—where M is a group IVb, Vb or VIb transition metal atom and X is a chalcogen atom, S, Se or Te—display a range of interesting physical properties (e.g. Wilson and Yoffe 1969, Mooser 1972–9) such as, for example, charge density wave structural instabilities (Williams 1976). Crucial to an understanding of the behaviour of these compounds is a knowledge of their electronic band structures. Angle-resolved electron spectroscopies enable us to probe these experimentally; information on the occupied valence bands is given by angle-resolved photoelectron spectroscopy (ARPES) (e.g. Smith 1978) whilst the dispersions of the unoccupied conduction bands above the Fermi level, E_F, can be followed using momentum (k)-resolved inverse photoelectron spectroscopy (KRIPES) (e.g. Smith 1988). The results of such experiments provide a critical test of calculated band structures and the applicability of the theoretical methods employed to produce them.

§ Present address: Physics and Chemistry of Solids Group, Cavendish Laboratory, Madingley Road, Cambridge CB3 0HE, UK.

0953-8984/91/070813 + 13 $03.50

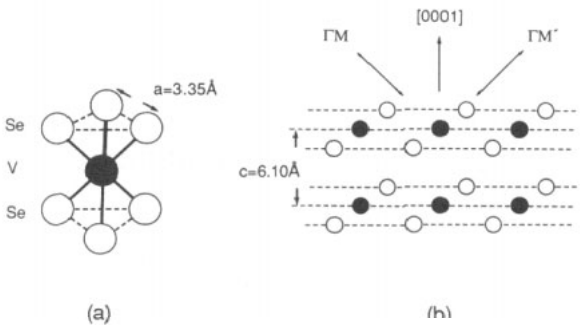

Figure 1. In the 1T crystal structure of VSe_2, the Se and V layers stack such that the V atoms are octahedrally coordinated by Se atoms (a). As discussed in the text, the three-fold symmetry results in two distinct 'ΓM' azimuths; these are defined relative to the crystal structure in (b), in which a {1120} plane of the crystal structure is shown.

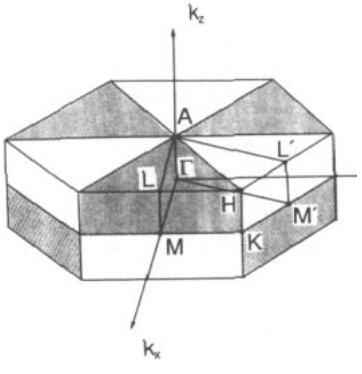

Figure 2. The Brillouin zone of the 1T, CdI_2 structure. Shaded and unshaded wedges are equivalent by symmetry on their surfaces and along their edges but are inequivalent in their interiors. Zone dimensions are $|\Gamma A| = 0.51$ Å^{-1}, $|\Gamma M| = 1.08$ Å^{-1}, $|\Gamma K| = 1.25$ Å^{-1}.

The weak interlayer interactions in TMDCs make them particularly amenable to such angle-resolved spectroscopic studies. From an experimental point of view, they cleave readily to produce clean, well-ordered surfaces. Also, interpretation of the data is relatively straightforward since only slight band dispersion normal to the layers is expected, thereby reducing the problem of the indeterminacy of the electron's component of momentum perpendicular to the surface, $k_\perp$ (Smith 1978).

The group Vb TMDC vanadium diselenide, VSe_2, has already been the subject of a number of ARPES studies, all yielding information on the experimental valence band energies and dispersions (Hughes *et al* 1980, Drude *et al* 1980, Johnson *et al* 1986). Combined with such data, optical reflectivity measurements (Bayliss and Liang 1984) can provide some information on the states lying above the Fermi level. More direct and detailed information though is given by KRIPES and we report the results of such a study in this paper. (A short account of this work has already appeared elsewhere (Law *et al* 1990).)

VSe_2 adopts the 1T, CdI_2 crystal structure (D^3_{3d} space group), the Se–V–Se sheet stacking sequence resulting in octahedral coordination of the V atoms by Se atoms. This crystal structure is depicted in figure 1, with the corresponding, relatively flat Brillouin zone being shown in figure 2. The overall three-fold symmetry of the 1T structure results

in asymmetry about the ΓKM plane of the Brillouin zone (Wooley and Wexler 1977) and two distinct 'ΓM' azimuths. These we shall denote as ΓM and ΓM', defined relative to the crystal structure as shown in figure 1. The ΓM (ΓM') azimuth is that in which the first neighbour Se atom lies beneath (above) the ΓM direction. (This notation is in keeping with that used by other workers, e.g. de Boer *et al* (1984).)

A variety of techniques have been used to calculate the theoretical band structure of VSe_2. Wooley and Wexler (1977) used the layer method, Zunger and Freeman (1979) performed a first-principles self-consistent (non-muffin tin) local density functional calculation and Myron (1980) employed the augmented plane wave method. All these calculations give qualitatively similar results but that of Zunger and Freeman (1979) (hereafter referred to as ZF) has been found to give the best overall agreement with ARPES data (Drube *et al* 1980, Johnson *et al* 1986) and optical reflectivity data (Bayliss and Liang 1984). Therefore, it is primarily with this calculation that we shall compare our KRIPES results.

The valence bands are formed from σ-type bonding combinations of Se 4p orbitals with some V 3d and 4p character; their antibonding σ^*-type counterparts lie about 7 eV higher in energy. Within this bonding–antibonding gap are found the V 3d-derived bands, ligand field split into t_{2g}-like (mainly d_{z^2}, d_{xy} and $d_{x^2-y^2}$) and e_g-like (mainly d_{xz} and d_{yz}) sub-bands. The trigonal distortion of the lattice ($c/a = 1.82$) further splits the lower energy 't_{2g}' sub-band with the singly-degenerate 'd_{z^2}'-like band being partially occupied to give the observed metallic behaviour. The unique ability of KRIPES to probe directly states lying between the Fermi level and the vacuum level makes it an ideal technique for studying the energies and splittings of these d bands. Indeed, the usefulness of the technique for studying the band-structures of TMDCs has already been demonstrated by other workers, notably Skibowski's group in Kiel who have carried out work on $TiSe_2$ (Drube *et al* 1984, 1987, Straub *et al* 1985), $TiTe_2$ (Drube *et al* 1987) and TaS_2 (Claessen *et al* 1990).

The layout of the paper is as follows. After giving experimental details in section 2, the normal incidence and off-normal incidence results are presented and discussed in section 3. In section 4, the variation of the intensity of photon emission with azimuthal angle of electron incidence is briefly considered. Conclusions are drawn in section 5.

2. Experimental details

The inverse photoemission measurements were made using the KRIPES grating spectrometer at Liverpool (Andrews 1988), an apparatus which operates in the isochromat mode. The photon flux emitted at a fixed photon energy is measured as the incident electron energy is scanned; total energy resolution is typically around 0.6 eV at 20 eV photon energy and momentum resolution is about 0.1 $Å^{-1}$. The electron gun and grating/photon detector combination are fixed so variation of the polar angle of incidence, θ, of the electron beam is achieved by rotation of the sample. For the data presented here, positive (negative) angles of incidence correspond to rotation of the sample towards (away from) the grating—see figure 3.

The VSe_2 samples, typically 3×3 mm^2 in size, were glued to copper mounting plates using a silver-filled conducting epoxy adhesive (Ablebond 36-2). To achieve *in vacuo* azimuthal rotation of the samples on the x, y, z manipulator, these copper plates were attached to a holder that could be azimuthally rotated in a crude, but effective, manner

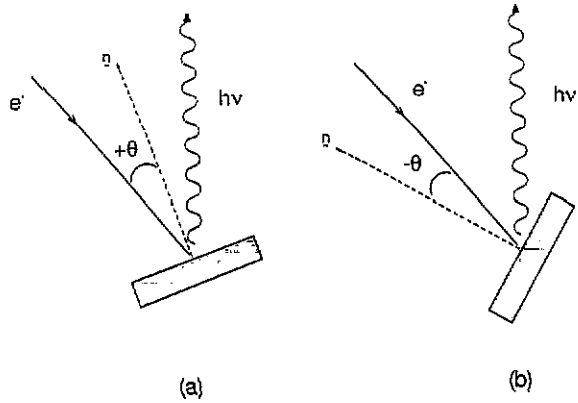

Figure 3. Definition of the angle of electron incidence, θ. Positive θ values (a) correspond to rotation of the sample normal, n, towards the grating. Negative θ values (b) correspond to rotation of the sample normal, n, away from the grating.

by use of a wobble stick. Clean surfaces were obtained by cleaving the samples in ultra-high vacua of better than 5×10^{-11} mbar.

Low energy electron diffraction (LEED) was used to determine the azimuthal orientation of the samples. The three-fold symmetry of the 1T structure reveals itself in the intensity of the first order LEED beams; depending on the incident electron energy these are more intense along either the ΓM or ΓM′ azimuth. By relating the observed LEED pattern to the intensity of photoemission from the occupied part of the 'd_{z^2}' band—which is known to be greater along the ΓM azimuth than the ΓM′ azimuth in related TMDCs whose orientation has been determined by x-ray diffraction (Smith and Traum 1975, de Boer *et al* 1984)—the ΓM and ΓM′ azimuths can be identified (Starnberg 1990). For example, for a primary beam energy of 67 eV the first-order beams are more intense along the ΓM azimuth. It should be noted that such considerations lead to the opposite assignment of the ΓM and ΓM′ azimuths to that given in our earlier paper (Law *et al* 1990).

3. Results and discussion

In order to determine band dispersions as a function of $k_\perp$ i.e. along ΓA, normal-incidence ($|k_\parallel| = 0$) spectra were recorded at photon energies between 17 and 28 eV. These are shown in figure 4; the spectra have been plotted to the same maximum intensity, after normalizing the measured photon flux to the incident electron charge.

Four distinct features are seen in the normal-incidence spectra: strong peaks at about 1 eV and about 3 eV above E_F, a weak peak at about 5 eV and a broad feature centred at about 8 eV and showing a threshold at about 6.5 eV. In addition, a shoulder is apparent on the high energy side of the ~1 eV peak in the 17 eV spectrum. All the peaks show less than 0.6 eV dispersion over the photon energy range studied, confirming the expected weak dispersion of the states along ΓA.

In order to reduce the features in the spectra of figure 4 to a plot of final-state energy, E, against $k_\perp$, a knowledge of the initial states involved is required. Usually some approximation to these has to be made since theoretical band structures rarely extend

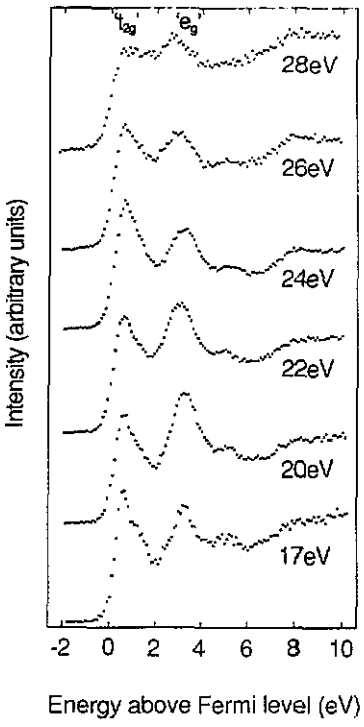

Figure 4. Normal-incidence isochromat KRIPES spectra recorded at photon energies between 17 and 28 eV.

to sufficiently high energies. Here we adopt a free-electron-like approximation for the initial states, as has been used previously for other TMDCs (Straub *et al* 1985, Drube *et al* 1987). $|k_\perp|$ is then given by:

$$|k_\perp| = (2m/\hbar^2)^{1/2}(\varepsilon + V_0)^{1/2}$$

where ε is the kinetic energy of the initial-state electron relative to the vacuum level, V_0 is the inner potential and m is the electron mass. Using a value of $V_0 = 10.2$ eV, i.e. placing the bottom of the free-electron-like band at the valence band minimum at Γ of the ZF calculation and using a value of 4.4 eV for the work function (Hughes *et al* 1980), gives the $E/k_\perp$ plot shown in figure 5; the data have been reduced to the first Brillouin zone by subtraction of the appropriate reciprocal lattice vector, $G = (003)$. For comparison, the theoretical bands of the ZF calculation are also given in this figure.

Three of the features can now be identified. The strong peaks at about 1 eV and about 3 eV arise from transitions into the V 3d-derived 't_{2g}'- and 'e_g'-like sub-bands respectively and the broad feature at about 8 eV results from transitions into the anti-bonding σ^*-type bands. The feature at about 5 eV, which cannot be so readily associated with any of the calculated bands, will be considered later after discussion of the d-band peak energies in both these normal-incidence data and the off-normal-incidence spectra.

Although a free-electron-like initial-state band is only an approximation, some confidence in its use is given by the fairly good agreement found between our data and the ZF calculation. The predicted upwards dispersion from Γ to A of the doubly degenerate Δ_3 'e_g' band is seen in our data, though the change in peak energy from

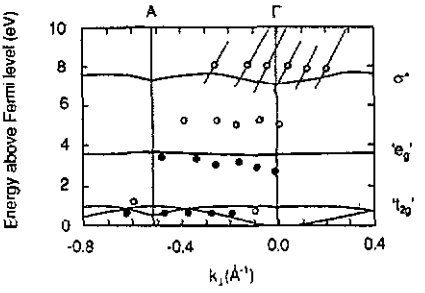

Figure 5. Features in the normal-incidence KRIPES spectra of figure 4 reduced to a final-state energy versus $k_\perp$ diagram assuming a free-electron-like initial-state band as discussed in the text. ●, strong features; ○, weak features. The width of the broad feature centred at about 8 eV is indicated by the straight lines. Superimposed for comparison are the calculated bands of Zunger and Freeman (1979).

2.7 eV in the 28 eV spectrum (close to Γ) to 3.3 eV in the 17 eV spectrum (near to A) implies a dispersion of about 0.6 eV, greater than the ~0.2 eV dispersion of the Γ_3^+–A_3^+ band predicted by ZF and the Δ_3 bandwidths of 0.2 and 0.3 eV calculated by Wooley and Wexler (1977) and Myron (1980) respectively. The experimental data also imply that the ZF calculation underestimates the binding energy of this Δ_3 band by about 0.6 eV, the experimental mid-point energy being 3.0 eV compared with 3.6 eV in the ZF calculation. On the other hand, the other calculations both overestimate the binding energy of this band by about 0.5 eV, their mid-point energies being about 2.5 eV. Interpretation of their optical reflectivity measurements led Bayliss and Liang (1984) to suggest that the d-band energies calculated by ZF needed to be lowered by 0.2–0.3 eV. Our results indicate that for the 'e_g' band a somewhat greater increase in binding energy than this is required.

The trigonal distortion of the octahedral crystal structure splits the lower energy 't_{2g}' manifold into a singly degenerate Δ_1 (mainly 'd_{z^2}') band and a doubly degenerate Δ_3 (mainly 'd_{xy}' and '$d_{x^2-y^2}$') band. The shoulder at about 1.2 eV in the 17 eV spectrum implies a value of about 0.6 eV for this splitting close to the A point, assuming the $|k_\perp|$ determination is not unreasonable. This experimental value is greater than the predicted A_3^+–A_1^+ splitting: ~0.2 eV in the ZF calculation, ~0.1 eV in the Wooley and Wexler (1977) calculation and ~0.3 eV in the Myron (1980) calculation. Interlayer interactions cause the Δ_3 and Δ_1 bands to cross over between A and Γ (Wooley and Wexler 1977), the Δ_1 band moving to just below E_F near the Γ point. Unfortunately we cannot follow these dispersions across the Brillouin zone as the experimental resolution deteriorates with increasing photon energy. However, the observed change in intensity of the ~1 eV peak with photon energy might, at least in part, be explained by this predicted band behaviour; the increase in intensity of this feature in the 24 eV spectrum, and subsequent decrease at higher photon energies, could result from the downward dispersion of the Δ_1 band through the Δ_3 band and to below E_F at Γ. In the ZF calculation the splitting at Γ (Γ_1^+–Γ_3^+) is 0.93 eV. This is larger than the value of about 0.3 eV found in the other calculations (Wooley and Wexler 1977, Myron 1980) but consistent with our data, assuming that the weak peak in the 28 eV spectrum represents the Γ_3^+ state and that the Γ_1^+ state lies just below E_F as indicated by photoemission (Hughes *et al* 1980, Drube *et al* 1980, Johnson *et al* 1986).

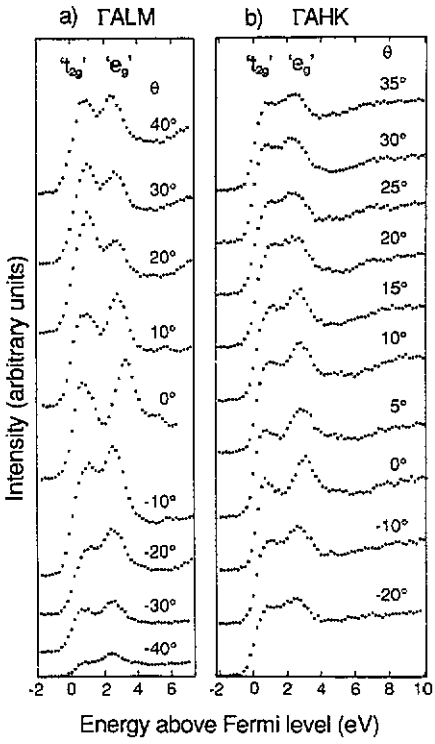

Figure 6. Off-normal-incidence 20 eV isochromat KRIPES spectra recorded in (a) the ΓALM plane and (b) the ΓAHK plane of the Brillouin zone.

The $k_\parallel$ dispersions of the features seen in the normal-incidence spectra were followed by recording 20 eV isochromat spectra at off-normal polar angles of electron incidence in the principal symmetry planes of the Brillouin zone, ΓALM and ΓAHK; these spectra are shown in figure 6. As for the normal-incidence spectra, the measured photon flux has been normalized to the incident electron charge. The ΓAHK spectra were recorded after the normal-incidence measurements shown in figure 4. Spectra obtained in this symmetry plane from another crystal immediately after cleaving gave the same peak energies but had a lower peak-to-background signal ratio due to an inferior quality cleave. The ΓALM spectra were obtained immediately after cleaving a third sample. For the spectra recorded in the ΓALM plane, positive (negative) polar angles correspond to electrons incident along the ΓM (ΓM′) azimuth, i.e. $k_\parallel$ in the ΓAL′M′ (ΓALM) plane. A photon energy of 20 eV was chosen primarily so that the initial-state energies involved in transitions to final states close to E_F would be the same as the final states populated in He I (21.2 eV)-excited photoemission from states just below E_F. It also represents something of a compromise between instrumental resolution and data acquisition time. Whilst the resolution is better at lower photon energies, the electron gun/grating combination is less efficient.

Features in the spectra of figure 6 have been reduced in the usual manner (Hughes and Liang 1973) to produce the $E/k_\parallel$ plots given in figure 7. We again include the theoretical bands of ZF in this figure; bands in both the ΓKM and AHL planes are given because KRIPES, like ARPES, tend to average over the height of the relatively flat Brillouin

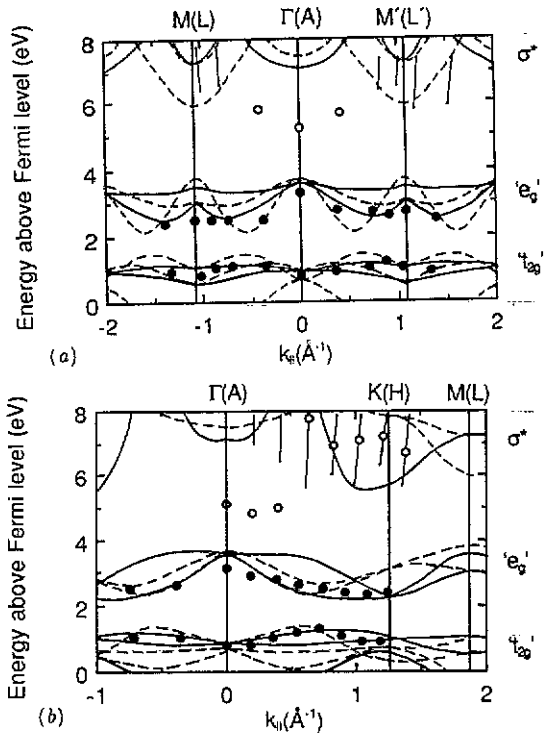

Figure 7. Final-state energy versus $k_{\parallel}$ diagrams for (a) features in ΓALM spectra and (b) features in ΓAHK spectra. ●, strong features; ○, weak features. The width of the broad feature above about 6 eV is indicated by the straight lines. Superimposed are the calculated bands of Zunger and Freeman (1979) for the ΓKM (———) and AHL (– – –) planes of the Brillouin zone.

zones of TMDCs. Band dispersions along the edges of the ΓALM and ΓAL'M' planes are identical because the band structure is six-fold symmetric on the mid-plane, ΓKM, and top face, AHL, of the Brillouin zone. However, small differences are possible away from the edges. This might account for the slight differences in the 'e_g' peak energy seen in spectra recorded with the electrons incident in the ΓM azimuth and in the ΓM' azimuth.

In table 1 we compare our experimental critical point energies with those found in the three theoretical band structures. Overall, the ZF calculation shows the best agreement with our data. For example, only ZF correctly predict the overall downward dispersion of the 'e_g' sub-band from Γ(A) to M(L). Also, the observed small dispersion, ~0.4 eV, of the 't_{2g}' peak in the ΓALM plane favours the ZF calculation. Both Wooley and Wexler (1977) and Myron (1980) predict an upwards dispersion of about 1–1.5 eV from Γ(A) to M(L) of the 'd_{xy}' and '$d_{x^2-y^2}$' components of the 't_{2g}' sub-band.

At the zone centre, the experimental bands are observed at higher energies than predicted by Wooley and Wexler (1977) and Myron (1980). Whilst 'self-energy' effects would shift the experimental bands to higher energies than predicted by 'ground-state' calculations, such effects are expected to be less important for a metallic sample, such as VSe_2, than for semiconducting or semimetallic samples (e.g. Himpsel 1990). Anyway, a detailed discussion of such effects here is precluded by the wide variation in the 'ground-state' energies predicted by the three calculations.

Table 1. Critical point energies of the unoccupied bands of VSe_2 predicted by the band-structure calculations of Wooley and Wexler (1977), Zunger and Freeman (1979) and Myron (1980), together with the experimental values determined in this KRIPES study. The bands in the left-hand column are given in order of increasing Γ, M and K critical-point energies in the Zunger and Freeman (1979) calculation. (Note that the order of the components of the 't_{2g}' and 'e_g' sub-bands along ML differs in the Myron (1980) calculation.) The error in the experimental energies is ±0.1 eV.

Critical point	Wooley and Wexler (1977)	Zunger and Freeman (1979)	Myron (1980)	KRIPES This work
t_{2g} $\Gamma_1^+ (A_1^+)$	~0.0 (0.3)	~0.0 (0.9)	−0.1 (0.6)	−0.1† (1.2)
t_{2g} $\Gamma_3^+ (A_3^+)$	0.2 (0.2)	0.9 (0.7)	0.3 (0.3)	0.8 (0.6)
e_g $\Gamma_3^+ (A_3^+)$	2.4 (2.6)	3.5 (3.7)	2.3 (2.6)	2.7 (3.3)
$\Gamma_1^+ (A_2^-)$	4.5 (5.7)	7.1 (7.5)	— —	>6.8 (>7.2)
t_{2g} $M_1^+ (L_1^+)$	1.2 (1.3)	0.6 (0.6)	1.7 (1.8)	0.9
t_{2g} $M_2^+ (L_2^+)$	1.2 (1.3)	1.1 (1.0)	1.5 (1.5)	
e_g $M_1^+ (L_1^+)$	2.4 (3.1)	3.0 (3.7)	2.8 (3.5)	2.6
e_g $M_2^+ (L_2^-)$	2.6 (2.3)	3.5 (3.0)	2.7 (2.4)	
$M_2^- (L_2^-)$	5.2 (3.6)	7.3 (6.0)	— (3.5)	>6.0
t_{2g} $K_1 (H_1)$	0.7 (0.8)	0.5 (0.3)	1.1 (1.1)	0.9
t_{2g} $K_3 (H_3)$	1.0 (0.6)	1.0 (0.7)	1.2 (0.7)	
e_g $K_3 (H_3)$	1.9 (2.4)	2.3 (3.1)	2.2 (2.8)	2.4
$K_2 (H_3)$‡	4.6 (5.6)	5.7 (7.8)	— —	>6.0

† This value is extracted from published ARPES results (Johnson *et al* 1986).

‡ In the Wooley and Wexler (1977) calculation this lowest energy s/p band has $K_1 (H_2)$ symmetry.

By taking the difference between mid-point energies of the observed dispersions of the 't_{2g}' and 'e_g' bands, we can obtain an experimental estimate of the ligand-field splitting. The value obtained—1.8 eV—compares favourably with the value of 1.7 eV quoted by ZF for the centre-of-gravity splitting of these bands and with the value of 1.6 eV estimated by Webb and Williams (1975) from soft-x-ray appearance potential spectroscopy (SXAPS) data.

Using ARPES, Johnson *et al* (1986) demonstrated that the p and d valence bands overlap at Γ to produce a small hole pocket. Although we are not able to detect this with the present experimental resolution, we can perhaps infer that a band crosses E_F by inspecting the photon emission intensity at the Fermi level, $I(E_F)$, as a function of $k_\parallel$. This information is plotted in figure 8. (The asymmetry in the intensity at positive and negative $k_\parallel$ in the ΓALM plane is considered in section 4.)

In the ΓAHK plane, a small increase in $I(E_F)$ is seen at $|k_\parallel| \sim 0.2$ Å^{-1} ($\theta = +5°$), where a decrease in the intensity of the 'd_{z^2}' photoemission peak due to hybridization with the p band was seen by Johnson *et al* (1986). $I(E_F)$ also increases at $|k_\parallel| \sim 0.8$ Å^{-1}

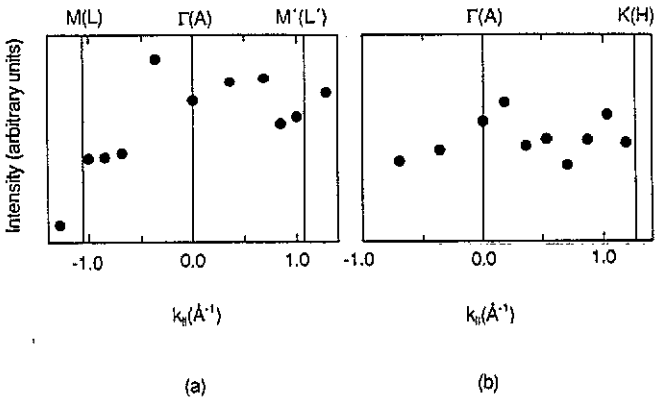

Figure 8. The measured photon emission intensity at the Fermi level plotted as a function of $k_{\parallel}$ for (a) ΓALM spectra and (b) ΓAHK spectra. The intensity scale is the same for both plots.

in the ΓAHK plane, where the 'd_{z^2}' band is predicted to disperse above E_F along ΓK. Along ΓAL'M', the decrease in $I(E_F)$ seen around M' (L') reflects the fact that the 'd_{z^2}' band has moved further below E_F to a minimum at the L critical point.

We now consider the two higher energy features in the spectra, namely the weak peak at about 5 eV and the broad feature at about 8 eV.

The ~5 eV peak shows little dispersion in the normal-incidence spectra i.e. along ΓA. In the off-normal incidence data, however, the feature moves upwards in both the ΓAHK and ΓALM planes, merging into the broad, higher energy feature for $|\theta| > 20°$. A similar peak was seen for $TiTe_2$ and $TiSe_2$ by Drube *et al* (1987) and interpreted as the $n = 1$ image potential state, lying 0.7 eV below the vacuum level and having an effective mass $m^*/m = 1.5$ in the case of $TiTe_2$. Although we were not able to measure the work function of our sample, the value of 4.4 eV determined by Hughes *et al* (1980) from the secondary electron cut-off of ARPES spectra, and confirmed by Starnberg (1990) using the same method, would rule out identification of this feature as an image potential state since it would lie about 0.6 eV above the vacuum level.

The ZF and Wooley and Wexler (1977) calculations show considerable differences in the energies of the σ^* bands, which are derived primarily from the V 4s and 4p orbitals. (The Myron (1980) calculation does not extend to such energies.) The lowest σ^* band at Γ lies at about 7 eV above E_F in the ZF calculation and at about 4.5 eV in the Wooley and Wexler (1977) calculation. Therefore, the presence of a feature at about 5 eV in the spectra could indicate inaccuracies in the ZF calculation. On the other hand, these s/p_z-derived bands are predicted to show an upwards dispersion of about 1 eV along ΓA; this is not seen in the normal-incidence data. The observed lack of $k_{\perp}$ dispersion suggests another possibility: the feature could result from transitions into a surface resonance lying between the d bands and the σ^* bands. However, although the sample was not deliberately dosed to check the sensitivity of this feature to surface contamination, it apparently decreased in intensity no faster than other features in the spectra as the sample gradually became contaminated over time. Therefore, the origin of this feature must remain somewhat uncertain.

Tentative identification of the ~5 eV feature as a surface resonance within the d-band–σ^*-band gap is supported by the good agreement found between the broad feature

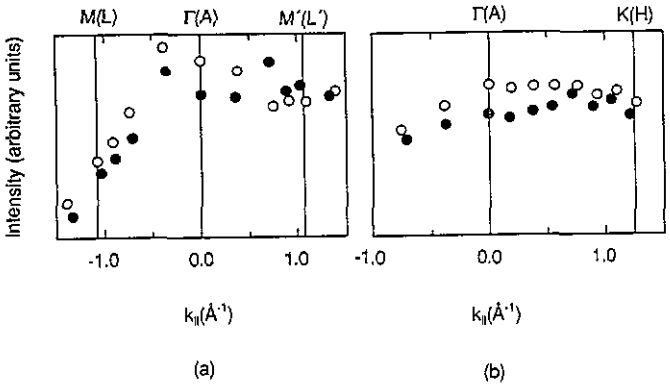

Figure 9. The measured photon emission intensity (peak height) of the 't_{2g}' peak (●) and the 'e_g' peak (○) plotted as a function of $k_\parallel$ for (a) the ΓALM spectra and (b) the ΓAHK spectra. The intensity scale is the same for both plots.

centred at about 8 eV, and having a threshold at around 6 eV near the Brillouin zone boundaries, and the energies of the σ^* bands in the ZF calculation. For example, this broad feature shows the expected general downward dispersion from Γ(A) to H(K). Such an interpretation of our data gives little support for the suggestion of Bayliss and Liang (1984), based on their optical reflectivity data, that the energy of the σ^* bands is underestimated by 1–2 eV near M and K in the ZF calculation.

4. d-band intensities

In this section the intensity of photon emission resulting from transitions into the d-bands is briefly considered. Inspection of the off-normal-incidence spectra reveals different d-band peak intensities along the two distinct ΓM azimuths; this is illustrated in figure 9, where the heights of the 't_{2g}' and 'e_g' peaks are plotted against $k_\parallel$ for both principal symmetry planes. (A slight difference in intensities at positive and negative angles of incidence is evident also in the ΓAHK data, indicating that a small experimental intensity asymmetry arises from the different photon collection geometries—see figure 3.) Such an asymmetry in the photon emission intensity between the ΓM and ΓM' azimuths—which reflects the three-fold symmetry of the crystal structure—has also recently been observed by Drube *et al* (1987) in their KRIPES study of $TiTe_2$ and by Claessen *et al* (1990) for 1T-TaS_2.

Anisotropy in the intensity of *photoemission* from the *occupied* d band of 1T-$TaSe_2$ and 1T-TaS_2 as a function of azimuth angle was observed by Smith and co-workers (Smith and Traum 1975, Traum and Smith 1975a, b, Smith *et al* 1976) in the early days of angle-resolved photoemission. The effect has since been seen for a number of TMDCs. In the case of VSe_2 (Hughes *et al* 1980, Drube *et al* 1980, Johnson *et al* 1986, Starnberg 1990), the intensity of He I (21.2 eV)-excited photoemission from the occupied portion of the 'd_{z^2}' band is greater along the ΓM azimuth ($k_\parallel$ in the ΓALM plane) than along the ΓM' azimuth ($k_\parallel$ in the ΓAL'M' plane). This is in the same sense as the asymmetry seen for 1T-TaS_2 by Smith and Traum (1975). Noting that the stronger emission was along directions corresponding to electron trajectories that avoided nearest-neighbour chalcogen atoms in the top layer, they speculated that this might be a shadowing effect, the

chalcogen atoms in the top layer being opaque to electrons emitted from the metal atoms. After further work at different photon energies and polarizations (Traum and Smith 1975a, b, Smith *et al* 1976), they abandoned this suggestion.

Another explanation for the observed three-fold symmetry involved the modulating effect of the momentum matrix element of the optical transition, the azimuthal intensity pattern then reflecting the angular dependence of the d orbitals involved. Smith and Traum (1975) showed that the pattern observed at $h\nu = 10.2$ eV was consistent with the angular orientation of t_{2g} rather than e_g orbitals. However, to account for fine structure in the azimuthal patterns, Liebsch (1976) found it necessary to include multiple scattering in the final state.

With KRIPES both the 't_{2g}'-like and 'e_g'-like sub-bands are probed. The matrix element effects discussed by Smith and co-workers would be expected to give different azimuthal intensity behaviour for these sub-bands since they have different spatial distributions. Indeed, such effects probably account for the different relative intensities of the 't_{2g}' and 'e_g' peaks along ΓM and ΓM' (compare, for example, the +20° and −20° spectra in figure 6(*a*)). However, the absolute intensity of photon emission resulting from transitions into both d sub-bands is greater for electrons incident along the ΓM azimuth ($k_\parallel$ in the ΓAL'M' plane) than for electrons incident along the ΓM' azimuth ($k_\parallel$ in the ΓALM plane), suggesting that initial-state effects are important.

It is difficult to draw many conclusions from our somewhat limited data set and further experimental and theoretical work is clearly required. For example, in order to follow more closely the intensity changes as a function of polar angle of incidence, it would be desirable to rotate the electron gun rather than the sample and so keep fixed the angle at which the photons are collected. With the present arrangement this varies as the sample is rotated, so changing the polarization weighting of the light detected.

5. Conclusion

By application of the inverse photoemission technique, we have been able to elucidate the essential features of the unoccupied band structure of vanadium diselenide up to about 10 eV above the Fermi level. Normal-incidence spectra recorded over a range of photon energies and off-normal-incidence spectra recorded at 20 eV photon energy give information on the dispersion of bands as a function of $k_\perp$ and $k_\parallel$ respectively.

Of the three published theoretical band structures of this material, that of Zunger and Freeman (1979) is found to give the best overall agreement with our experimental findings. It predicts fairly well the energies and ligand-field splitting of the 't_{2g}' amd 'e_g' d sub-bands, as well as the general trends in their dispersions along the principal symmetry directions of the Brillouin zone. Good agreement is also found for the higher-lying s/p conduction bands at about 6 eV and above. However, within this framework, a non-$k_\perp$-dependent peak at about 5 eV has to be tentatively assigned to a surface resonance lying between the d and s/p bands.

Whilst our data support the suggestion of Bayliss and Liang (1984) that the d sub-band energies may be underestimated by about 0.2 eV in the Zunger and Freeman calculation, at least in the case of the 'e_g' band, we find no support for their suggestion that the s/p band energies are underestimated by about 1–2 eV, unless the peak seen at about 5 eV is associated with a bulk band.

An earlier KRIPES study of the group IVb TMDC, $TiSe_2$ (Drube *et al* 1984, 1987, Straub *et al* 1985), also favoured a Zunger and Freeman band structure calculation (Zunger and

Freeman 1978). Our results thus provide further confidence in the ability of their local-density-functional methods to produce realistic band structures for TMDCs. Obviously, though, most of the interesting physics of these materials involves states around the Fermi level. Whilst KRIPES is clearly a very valuable technique for elucidating general details of the unoccupied band structures of TMDCs, a considerable improvement in experimental resolution will be required before the technique can provide the same detailed information on the states just above E_F as is provided by high-resolution ARPES studies of the states just below E_F (e.g. Anderson *et al* 1985, Johnson *et al* 1986). Only then will it be possible to test fully the predictive power of theory in this region of interest.

Acknowledgments

We are grateful to the UK Science and Engineering Research Council for financial support and to Mrs S Nulsen for preparing the samples. ARL wishes to acknowledge Drs H I Starnberg, M T Johnson and I R Collins for helpful and stimulating discussions and correspondence, and Mr J Murray for expert technical assistance.

References

Anderson O, Manzke R and Skibowski M 1985 *Phys. Rev. Lett.* **55** 2188
Andrews P T 1988 *Vacuum* **38** 257
Bayliss S C and Liang W Y 1984 *J. Phys. C: Solid State Phys.* **17** 2193
Claessen R, Burandt B, Carstensen H and Skibowski M 1990 *Phys. Rev.* B **41** 8270
de Boer D K G, van Bruggen C F, Bus G W, Coehoorn R, Haas C, Sawatzky G A, Myron H W, Norman D and Padmore H 1984 *Phys. Rev.* B **29** 6797
Drube W, Karschnick G, Skibowski M, Thies R and Völkert K 1980 *J. Phys. Soc. Japan* **49** Suppl. A 137
Drube W, Schäfer I, Karschnick G and Skibowski M 1984 *Phys. Rev.* B **30** 6248
Drube W, Schäfer I and Skibowski M 1987 *J. Phys. C: Solid State Phys.* **20** 4201
Himpsel F J 1990 *Surf. Sci. Rep.* **12** 1
Hughes H P and Liang W Y 1973 *J. Phys. C: Solid State Phys.* **6** 1684
Hughes H P, Webb C and Williams P M 1980 *J. Phys. C: Solid State Phys.* **13** 1125
Johnson M T 1988 private communication
Johnson M T, Starnberg H I and Hughes H P 1986 *J. Phys. C: Solid State Phys.* **19** L451
Law A R, Andrews P T and Hughes H P 1990 *Vacuum* **41** 553
Liebsch A 1976 *Solid State Commun.* **19** 1193
Mooser E 1972–9 *Physics and Chemistry of Materials with Layered Structures* vol 1–6 (Dordrecht: Reidel)
Myron H W 1980 *Physica* **99**B 243
Smith N V 1978 *Photoemission from Solids I* (*Topics in Applied Physics* 26) ed M Cardona and L Ley (Berlin: Springer) ch 6
—— 1988 *Rep. Prog. Phys.* **51** 1227
Smith N V and Traum M M 1975 *Phys. Rev.* B **11** 2087
Smith N V, Traum M M, Knapp J A, Anderson J and Lapeyre G J 1976 *Phys. Rev.* B **13** 4462
Starnberg H I 1990 private communication
Straub D, Skibowski M, Himpsel F J and Drube W 1985 *Phys. Rev.* B **31** 8254
Traum M M and Smith N V 1975a *Phys. Lett.* **54A** 439
—— 1975b *Surf. Sci.* **53** 121
Webb C and Williams P M 1975 *Phys. Rev.* B **11** 2082
Williams P M 1976 *Crystallography and Crystal Chemistry of Materials with Layered Structures* ed F Lévy (Dordrecht: Reidel) pp 51–92
Wilson J A and Yoffe A D 1969 *Adv. Phys.* **18** 193
Wooley A M and Wexler G 1977 *J. Phys. C: Solid State Phys.* **10** 2601
Zunger A and Freeman A J 1978 *Phys. Rev.* B **17** 1839
—— 1979 *Phys. Rev.* B **19** 6001